

Monte Carlo Adaptive Resolution Simulation of Multicomponent Molecular Liquids

Raffaello Potestio,^{1,*} Pep Español,² Rafael Delgado-Buscalioni,³ Ralf Everaers,⁴ Kurt Kremer,¹ and Davide Donadio¹

¹Max-Planck-Institut für Polymerforschung, Ackermannweg 10, 55128 Mainz, Germany

²Departamento de Física Fundamental, Facultad de Ciencias (UNED), Avenida Senda del Rey 9, 28040 Madrid, Spain

³Departamento de Física Teórica de la Materia Condensada and IFIMAC, Universidad Autónoma de Madrid, Campus de Cantoblanco, 28049 Madrid, Spain

⁴Laboratoire de Physique et Centre Blaise Pascal, École Normale Supérieure de Lyon, CNRS UMR5672, 46 Allée d'Italie, 69364 Lyon, France

(Received 16 April 2013; published 8 August 2013)

Complex soft matter systems can be efficiently studied with the help of adaptive resolution simulation methods, concurrently employing two levels of resolution in different regions of the simulation domain. The nonmatching properties of high- and low-resolution models, however, lead to thermodynamic imbalances between the system's subdomains. Such inhomogeneities can be healed by appropriate compensation forces, whose calculation requires nontrivial iterative procedures. In this work we employ the recently developed Hamiltonian adaptive resolution simulation method to perform Monte Carlo simulations of a binary mixture, and propose an efficient scheme, based on Kirkwood thermodynamic integration, to regulate the thermodynamic balance of multicomponent systems.

DOI: 10.1103/PhysRevLett.111.060601

PACS numbers: 05.10.Ln, 36.20.Ey, 61.20.Ja, 82.20.Wt

Soft matter systems often display an inherently multiscale nature. Because of this interplay of length and time scales, a unique level of description is not sufficient: a fully atomistic (AT) simulation would be too computationally expensive, while coarse-grained (CG) models [1–5] would lack the necessary detail to account for local interactions. In recent years, methods have been developed that couple models with different resolutions in a single simulation, where a small “important” region is treated at the full atomistic level, while in the surrounding region a coarser model is used. Examples of successful applications of this approach are mixed quantum mechanics and molecular mechanics (QM-MM) schemes [6–10], also employed to study crack propagation in hard matter [11–15], and the extension to complex fluids [16–27], where diffusion plays a crucial role. Adaptive resolution methods unite the advantageous simplicity and general versatility of CG models with the chemical specificity of higher resolution AT descriptions. To employ them successfully one needs to correct the thermodynamic mismatch that usually exists between models at different resolution. In the adaptive resolution simulation (AdResS) scheme [18–20,23,28] this is achieved with the help of a thermodynamic force [21,22] numerically obtained by an iterative procedure, which can become involved for multicomponent systems [25]. Here we tackle this problem using the recently developed Hamiltonian AdResS [26] (H-AdResS) and its tight connection to Kirkwood thermodynamic integration (TI) [29]. Our goal is twofold: first, we demonstrate the possibility to perform Monte Carlo (MC) simulations of a nontrivial double-resolution system using H-AdResS, formerly established in the framework of molecular dynamics (MD) [26]. Second, we describe a strategy to obtain in a single computationally efficient calculation that the

potential energy functions required to regulate the thermodynamic balance between AT and CG regions for multicomponent mixtures.

H-AdResS [26] is formulated in terms of a global Hamiltonian H , similar in spirit to the one used in TI [29]. In the H-AdResS Hamiltonian the total intermolecular energy of each molecule is weighted with a sigmoid function $\lambda(\mathbf{R})$, that depends on the center-of-mass coordinate \mathbf{R} of the molecule and ranges from 0 (purely CG) to 1 (purely AT):

$$H = K + V^{\text{int}} + \sum_a [\lambda_a V_a^{\text{AT}} + (1 - \lambda_a) V_a^{\text{CG}}], \quad (1)$$

$$V_a^{\text{AT}} = \frac{1}{2} \sum_{a' \neq a} \sum_{ij} V_{ai;a'j}^{\text{AT}}, \quad V_a^{\text{CG}} = \frac{1}{2} \sum_{a' \neq a} V_{aa'}^{\text{CG}},$$

where i, j are atom indices, $\lambda_a = \lambda(\mathbf{R}_a)$, K is the all-atom kinetic energy and V^{int} is the intramolecular interaction. If the Hamiltonian in Eq. (1) is straightforwardly used in a simulation, the difference in chemical potential between the AT and CG resolutions determines a density and pressure imbalance between the two regions of the system. In order to restore a flat density profile we introduced a compensation term $\Delta H(\lambda)$ in the Hamiltonian, which then reads $H_\Delta = H - \sum_a \Delta H(\lambda(\mathbf{R}_a))$. $\Delta H(\lambda)$ can be approximated with the Gibbs free energy difference per molecule (chemical potential) $\Delta G/N$, as obtained from a TI of a homogeneous system, performed in the canonical ensemble [26]:

$$\Delta H(\lambda) \equiv \frac{\Delta G(\lambda)}{N} = \frac{\Delta F(\lambda)}{N} + \frac{\Delta p(\lambda)}{\rho^*}, \quad (2)$$

$$\Delta F(\lambda) = \int_0^\lambda d\lambda' \langle [V^{\text{AT}} - V^{\text{CG}}] \rangle_{\lambda'},$$

where $\rho^* \equiv N/V$ is the reference molecular number density and $\Delta p(\lambda) = p(\lambda) - p(0)$ is the pressure difference. The free energy compensation (FEC) strategy, defined by Eq. (2), can be extended to multicomponent systems. To illustrate this idea we consider a molecular liquid composed by two types of molecules, A and B , indexed with a and b , respectively. The corresponding H-AdResS Hamiltonian for this system reads

$$H^{\text{MIX}} = K + V^{\text{int}} + \sum_{a \in A} [\lambda_a V_a^{\text{AT}} + (1 - \lambda_a) V_a^{\text{CG}}] + \sum_{b \in B} [\lambda_b V_b^{\text{AT}} + (1 - \lambda_b) V_b^{\text{CG}}], \quad (3)$$

with $\lambda_a = \lambda(\mathbf{R}_a)$ and $\lambda_b = \lambda(\mathbf{R}_b)$. The intermolecular potential energy terms are given by the following expressions:

$$\begin{aligned} V_a^{\text{AT}} &= \frac{1}{2} \left[\sum_{\substack{a' \in A \\ a' \neq a}} \sum_{ij} V[AA]_{ai;a'j}^{\text{AT}} + \sum_{b \in B} \sum_{ij} V[AB]_{ai;b j}^{\text{AT}} \right], \\ V_a^{\text{CG}} &= \frac{1}{2} \left[\sum_{\substack{a' \in A \\ a' \neq a}} V[AA]_{aa'}^{\text{CG}} + \sum_{b \in B} V[AB]_{ab}^{\text{CG}} \right], \\ V_b^{\text{AT}} &= \frac{1}{2} \left[\sum_{\substack{b' \in B \\ b' \neq b}} \sum_{ij} V[BB]_{bi;b'j}^{\text{AT}} + \sum_{a \in A} \sum_{ij} V[AB]_{bi;a j}^{\text{AT}} \right], \\ V_b^{\text{CG}} &= \frac{1}{2} \left[\sum_{\substack{b' \in B \\ b' \neq b}} V[BB]_{bb'}^{\text{CG}} + \sum_{a \in A} V[AB]_{ba}^{\text{CG}} \right], \end{aligned} \quad (4)$$

where $V[XY]$ is the nonbonded interaction between a molecule of type X and a molecule of type Y , with $X, Y = A, B$, and the indices i, j label the atoms.

In analogy with one-component systems we introduce a FEC term for each species to compensate for the free energy difference between the AT and the CG regions

$$H_{\Delta}^{\text{MIX}} = H^{\text{MIX}} - \sum_{a \in A} \Delta H_A(\lambda_a) - \sum_{b \in B} \Delta H_B(\lambda_b), \quad (5)$$

An ansatz for the compensation term of a given species $k = a, b$ can be obtained from TI as follows:

$$\begin{aligned} \Delta H_k(\lambda) &= \frac{\Delta F_k(\lambda)}{N_k} + \frac{\Delta p_k(\lambda)}{\rho_k^*}, \\ \Delta F_k(\lambda) &= \int_0^\lambda d\lambda' \langle [V_k^{\text{AT}} - V_k^{\text{CG}}] \rangle_{\lambda'}, \\ \Delta p_k(\lambda) &= p_k(\lambda) - p_k(0), \end{aligned} \quad (6)$$

where the N_k , $\rho_k^* \equiv N_k/V$ and p_k are, respectively, the number of molecules, the reference partial density and the partial virial pressure of species k (see the Supplemental Material [30]). We stress that all the quantities in Eq. (6) can be computed in a single TI of the mixture from AT to CG at the concentration of interest, irrespective of the

number of species. All the cross interactions between different types of molecules are automatically included in the free energy contribution of each species (details in the Supplemental Material [30]). Additionally, the free energy compensation $\Delta H_k(\lambda)$ is an intensive quantity and does not depend on the specific geometry of the H-AdResS setup. It is therefore possible to perform the TI in a relatively small system, provided that it is statistically representative; i.e., finite size effects are negligible.

A MC adaptive resolution simulation approach was formerly developed [31] by introducing a “dual-resolution partition function,” in which the resolution of a given molecule is a stochastic variable that depends on its position in space. Although physically sound, this approach cannot be rephrased in terms of a general Hamiltonian, as it is based on a modification of the partition function. In contrast H-AdResS is based on a dual-resolution Hamiltonian, and it can therefore be generalized to any statistical ensemble and simulation technique, thus including MC simulations. We implemented H-AdResS in a code based on the MC Metropolis algorithm [32]. Our code was tested on the homogeneous fluid used in Ref. [26] (data not shown), then used to validate the FEC method for mixtures, following Eqs. (5) and (6). Specifically, we considered two cases of binary mixtures of tetrahedral molecules, both made of four identical atoms (one of species A and one of species B), connected by quartic anharmonic bonds (see Ref. [18] and the Supplemental Material [30]). In case I the two molecular species are present in equal proportions (399 molecules of each type); atoms of the same species interact with a purely repulsive Weeks-Chandler-Andersen (WCA) potential, but the effective size of the B type is larger than the A type. In case II, 70% (558) A -type molecules and 30% (240) B -type molecules were used. In contrast with case I, the A - A and B - B WCA interactions are identical. In both cases the A - B interaction is a Lennard-Jones potential. The simulations were performed in the NVT ensemble at a temperature $T = 120$ K. The dimensions of the simulation box are $L_x = 3.684$ nm, $L_y = L_z = 1.50$ nm, with periodic boundary conditions in all directions. The AT-hybrid interface and the hybrid-CG interfaces are located at $d_h = \pm 0.15L_x$ and $d_h + s_h = \pm 0.3L_x$ from the box center, respectively. More details about the simulation setup are provided in the Supplemental Material [30].

As for the CG model one could choose among a number of different strategies [1–5], each of which targets a specific property of the underlying AT system. Here, instead, our intent is to show that H-AdResS and the FEC method allow a completely general and flexible coupling, irrespective of the specific CG potential used. To this end we use the *same* CG model in both cases, representing molecules as spherical particles with identical, purely repulsive WCA A - A , B - B , and A - B interactions [30]. The resulting thermodynamic mismatch in chemical potentials between AT

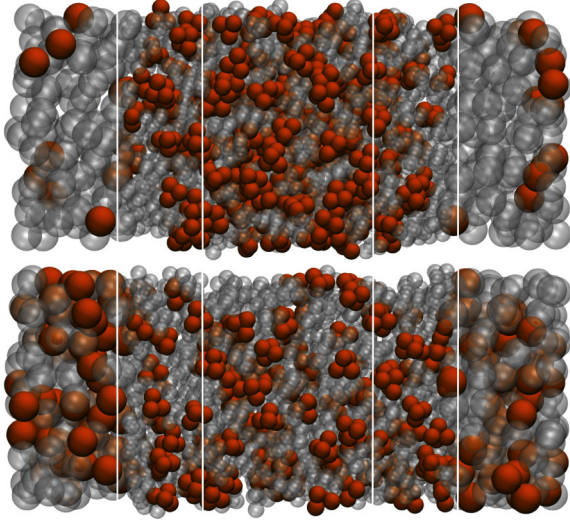


FIG. 1 (color online). Snapshots of a simulation of case II. Top panel: equilibrated configuration, without FEC. Bottom panel: equilibrated configuration, with FEC. The A-type atoms are represented in light gray (gray online), the B-type atoms in dark gray (orange online). Molecules in the coarse-grained (CG) region are represented as large spheres. White vertical lines mark the boundaries of the CG-hybrid and hybrid-atomistic regions.

and CG domains is particularly large in case II: simple visual inspection (Fig. 1, top) is in fact sufficient to detect a large accumulation of B molecules in the AT zone. Closer inspection of the density profiles (dotted lines in Fig. 2) also reveals significant deviations in case I. As a consequence, neither the total density nor the relative concentrations in the AT zone obtained using the uncompensated adaptive resolution Hamiltonian in Eq. (3) correspond to the reference atomistic system.

According to Eq. (6), we have determined the thermodynamic mismatch between the AT and the CG zone from two TI runs (one per case studied) where we switch the interactions of the mixtures from purely CG ($\lambda = 0$) to purely AT ($\lambda = 1$). The Helmholtz and Gibbs free energy differences per molecule between the CG and AT models as a function of the coupling parameter λ , computed for both species *simultaneously* in a single TI for each case, are shown in Fig. 3. In case I both Helmholtz and Gibbs free energy differences are similar in shape for the two species. The B-type molecules show a Gibbs free energy difference per particle $\Delta G_B/N_B \equiv [G_B(1) - G_B(0)]/N_B$ smaller in magnitude by $\sim 1k_B T$ than the A-type molecules. This difference can be attributed to the larger effective size of B-type atoms compared to A-type ones, which makes the size of the B-type AT molecules closer to that of the CG model. In case II the situation is remarkably different. In spite of the same interaction between molecules of the same type ($V[AA] \equiv V[BB]$), the uneven relative concentration of the two species determines a much larger free energy difference between the AT and CG models for the B

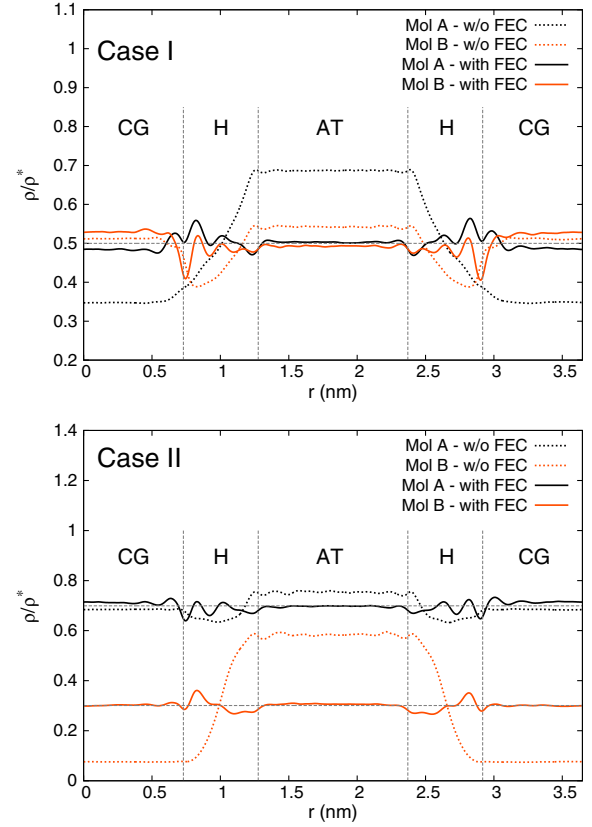


FIG. 2 (color online). Density profiles along the direction of resolution change, for case I (top) and case II (bottom). Dark lines (gray online) refer to A-type molecules, light lines (orange online) to B-type. Dotted lines: H-AdResS simulations without FEC; solid lines: with FEC. Vertical dashed lines indicate the boundaries between the AT, hybrid, and CG regions; horizontal dashed lines mark the reference value of the density (normalized to the total density) as expected in a fully atomistic simulation of the system.

type. In fact, the latter shows a Gibbs free energy difference per particle $|\Delta G_B/N_B| > 2|\Delta G_A/N_A|$. This is mainly due to the fact that the interaction between A and B types is attractive only in the AT representation, thus determining a lower chemical potential for the minority type (B) in the AT region. In addition, in both cases the sign of ΔG favors the densification of particles in the AT region, as can be seen in Fig. 2.

To counterbalance the mismatch in chemical potentials we introduce a FEC in the H-AdResS Hamiltonian according to Eq. (5), using the free energy functions shown in Fig. 3. The resulting density profiles (solid lines in Fig. 2) demonstrate the success of the procedure: in both case I and II the densities of the two species attain, in the AT region, the same values that would be observed in a fully atomistic simulation (for case II see also Fig. 1 bottom); also, the pairwise correlation functions in the AT region of both cases perfectly superimpose to the all-atom reference (see the Supplemental Material [30]). In particular, it is

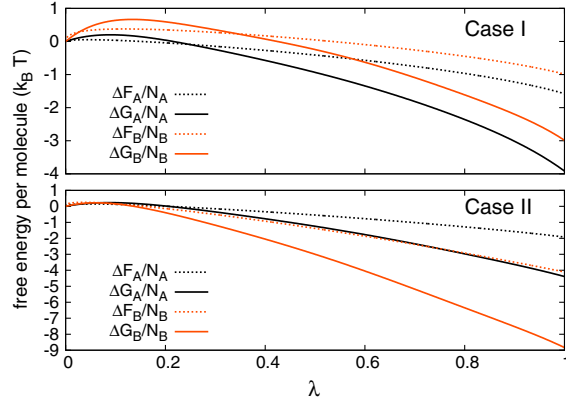


FIG. 3 (color online). Free energy differences per molecule between the AT and CG models as a function of the mixing parameter for case I (top) and case II (bottom). The Helmholtz free energy is represented by the dotted lines, the Gibbs free energy by the solid lines. Dark lines (gray online) refer to A-type molecules, light lines (orange online) to B-type.

remarkable that the simple FEC strategy fixed the density of B-type molecules in case II, where the free energy difference per particle between the AT and the CG representations span over one order of magnitude. In the CG region of case I a small ($\sim 3\%$) deviation from the reference can be observed, due to the depletion in the hybrid region typical of adaptive resolution simulations [18,21,22]. These density fluctuations are due to correlations between close-by molecules at different resolutions, which the FEC method, based on TI simulation where λ is the same for all molecules, cannot capture. These ripples, however, affect only the hybrid region (see Fig. 2), and can be leveled out employing iterative methods [22] to correct the FEC functions. A further validation of the effectiveness of the FEC method is provided in case III, where we performed the simulation of a system analogous to that of case I put in contact with a fixed, attractive wall. The latter is implemented as a Lennard-Jones potential acting in the same way on all the molecules, and depends on the distance between each atom and the wall. This potential has the same σ as the A-B interaction, but is four times stronger. In this case, only the subregion of the system close to the wall is treated at the atomistic level, and the same FEC's used for the homogeneous system were employed (details in the Supplemental Material [30]). In Fig. 4 we report the results obtained from this simulation: for both molecular species the density profiles superimpose perfectly on the reference, calculated from a fully atomistic simulation.

Finally, we mention two technical but relevant aspects of the dual-resolution approach, namely the sampling efficiency and the computational speedup. Using a CG model with softer interactions compared to the AT model we enhance the acceptance rate of the MC moves, thus improving the sampling of the configurational space. Additionally, the reduction of the number of degrees of

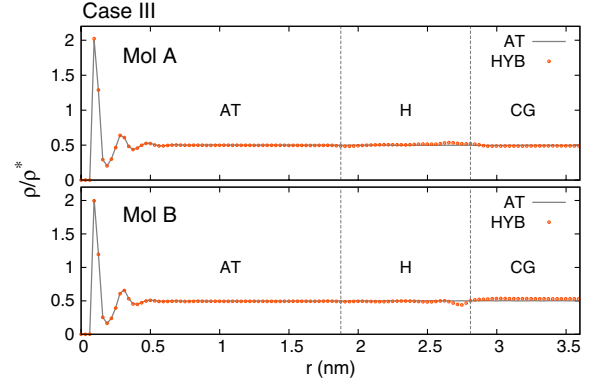


FIG. 4 (color online). Density profiles of the system of case III, where the mixture is put in contact with an attractive, fixed and nonpermeable wall. The results obtained in a H-AdResS simulation (orange points) perfectly superimpose on those of an analogous all-atom simulation (gray lines) for both A and B molecules (top and bottom panel, respectively).

freedom and the usage of simple CG potentials reduces the CPU time by a factor proportional to the level of coarse graining and to the system size L . For example, when a slab geometry is employed the computational gain grows linearly with L , while using a spherical AT region the speedup grows as L^3 (see the Supplemental Material [30]).

In summary, we employed the H-AdResS scheme to perform dual-resolution Monte Carlo simulations, and extended the FEC technique based on TI to regulate the density balance of AT and CG subregions, to the general case of a multicomponent system. This method allowed us to couple a two-component AT system to a CG potential, in which the two species are indistinguishable. In spite of the large free energy difference existing between these two models, the FEC approach effectively compensates large density imbalances. This procedure seamlessly accounts for the correlations between the densities of the various species. This work thus lays the theoretical background to drastically simplify the steps required to perform dual-resolution simulations of multicomponent systems, coupling an atomistic complex fluid to a simple CG model whose thermodynamic properties do not match the atomistic reference, still preserving the reference thermodynamic properties in the AT region. The limited impact of the choice of the CG potential can therefore be exploited to our advantage, for example by choosing CG potentials that facilitate either grand canonical particle insertion or particle switch in semi-grand-canonical simulations. Possible applications range from crystal growth [33,34] in an effective grand canonical ensemble to free energy calculations of biological systems in aqueous solutions [25]. H-AdResS also offers a promising route to fast calculations of variations of solvation free energy differences ($\Delta\Delta G$) due to changes in the composition and/or structure of a solvated macromolecule. In addition, the validation of H-AdResS in the framework of MC calculations is of

particular relevance for hybrid quantum-classical simulations [23,24] based on path integrals [35,36], where the inherently energy-based formulation makes it natural to employ MC methods.

The authors thank K. Kreis for a critical reading of the manuscript, and acknowledge hospitality at KITP, where this collaboration was initiated. This research was supported in part by the National Science Foundation under Grant No. NSF PHY11-25915. P.E. thanks the support of BIFI and the Ministry of Science and Innovation through Project No. FIS2010-22047-C05-03. R.D.-B. also thanks FIS2010-22047-C05-01 and the support of the “Comunidad de Madrid” via the Project No. MODELICO-CM (S2009/ESP-1691).

*potestio@mpip-mainz.mpg.de

- [1] K. Kremer, *Soft and Fragile Matter: Nonequilibrium Dynamics, Metastability and Flow*, SUSSP Proceedings Vol. 53 (IOP Publishing, London, 2000), p. 145.
- [2] C. Peter and K. Kremer, *Soft Matter* **5**, 4357 (2009).
- [3] N.A. van der Vegt, C. Peter, and K. Kremer, *Coarse-Graining of Condensed Phase and Biomolecular Systems* (CRC Press, London, 2009), p. 379.
- [4] C. Hijón, E. Vanden-Eijnden, R. Delgado-Buscalioni, and P. Español, *Faraday Discuss.* **144**, 301 (2010).
- [5] W. Noid, *Biomolecular Simulations*, Methods in Molecular Biology Vol. 924 (Humana Press, Totowa, NJ, 2013), p. 487.
- [6] A. Warshel and M. Levitt, *J. Mol. Biol.* **103**, 227 (1976).
- [7] J. Gao, *Rev. Comp. Chem.*, edited by K. Lipkowitz and D. Boyd (VCH, New York, 1995), Vol. 7, p. 119.
- [8] M. Svensson, S. Humbel, R. Froese, T. Matsubara, S. Sieber, and K. Morokuma, *J. Phys. Chem.* **100**, 19357 (1996).
- [9] P. Carloni, U. Rothlisberger, and M. Parrinello, *Acc. Chem. Res.* **35**, 455 (2002).
- [10] R. Buló, B. Ensing, J. Sikkema, and L. Visscher, *J. Chem. Theory Comput.* **5**, 2212 (2009).
- [11] R. Rudd and J. Broughton, *Phys. Status Solidi B* **217**, 251 (2000).
- [12] J. Rottler, S. Barsky, and M. O. Robbins, *Phys. Rev. Lett.* **89**, 148304 (2002).
- [13] G. Csanyi, T. Albaret, M. C. Payne, and A. De Vita, *Phys. Rev. Lett.* **93**, 175503 (2004).
- [14] D. Jiang and E. Carter, *Acta Mater.* **52**, 4801 (2004).
- [15] G. Lu, E. B. Tadmor, and E. Kaxiras, *Phys. Rev. B* **73**, 024108 (2006).
- [16] A. Heyden and D. G. Truhlar, *J. Chem. Theory Comput.* **4**, 217 (2008).
- [17] J. H. Park and A. Heyden, *Mol. Simul.* **35**, 962 (2009).
- [18] M. Praprotnik, L. Delle Site, and K. Kremer, *J. Chem. Phys.* **123**, 224106 (2005).
- [19] B. Ensing, S. Nielsen, P. Moore, M. Klein, and M. Parrinello, *J. Chem. Theory Comput.* **3**, 1100 (2007).
- [20] M. Praprotnik, S. Poblete, L. Delle Site, and K. Kremer, *Phys. Rev. Lett.* **107**, 099801 (2011).
- [21] S. Poblete, M. Praprotnik, K. Kremer, and L. Delle Site, *J. Chem. Phys.* **132**, 114101 (2010).
- [22] S. Fritsch, S. Poblete, C. Junghans, G. Ciccotti, L. Delle Site, and K. Kremer, *Phys. Rev. Lett.* **108**, 170602 (2012).
- [23] A. B. Poma and L. Delle Site, *Phys. Rev. Lett.* **104**, 250201 (2010).
- [24] R. Potestio and L. Delle Site, *J. Chem. Phys.* **136**, 054101 (2012).
- [25] D. Mukherji, N. F. A. van der Vegt, and K. Kremer, *J. Chem. Theory Comput.* **8**, 3536 (2012).
- [26] R. Potestio, S. Fritsch, P. Español, R. Delgado-Buscalioni, K. Kremer, R. Everaers, and D. Donadio, *Phys. Rev. Lett.* **110**, 108301 (2013).
- [27] H. Wang, C. Hartmann, C. Schütte, and L. Delle Site, *Phys. Rev. X* **3**, 011018 (2013).
- [28] M. Praprotnik, L. Delle Site, and K. Kremer, *Annu. Rev. Phys. Chem.* **59**, 545 (2008).
- [29] J. Kirkwood, *J. Chem. Phys.* **3**, 300 (1935).
- [30] See Supplemental Material at <http://link.aps.org/supplemental/10.1103/PhysRevLett.111.060601> for details about the system and simulation setup.
- [31] C. F. Abrams, *J. Chem. Phys.* **123**, 234101 (2005).
- [32] N. Metropolis, A. Rosenbluth, M. Rosenbluth, A. Teller, and E. Teller, *J. Chem. Phys.* **21**, 1087 (1953).
- [33] M. Salvalaglio, T. Vetter, F. Giberti, M. Mazzotti, and M. Parrinello, *J. Am. Chem. Soc.* **134**, 17221 (2012).
- [34] S. Piana and J. Gale, *J. Am. Chem. Soc.* **127**, 1975 (2005).
- [35] R. Feynman and A. R. Hibbs, *Quantum Mechanics and Path Integrals* (McGraw-Hill, New York, 1965).
- [36] M. E. Tuckermann, *Statistical Mechanics: Theory and Molecular Simulation* (Oxford University Press, Oxford, 2010).